Supporting Material for Stylianidou, Kuwada, and Wiggins "Cytoplasmic dynamics reveal two modes of nucleoid-dependent mobility."

SUPPORTING FIGURES

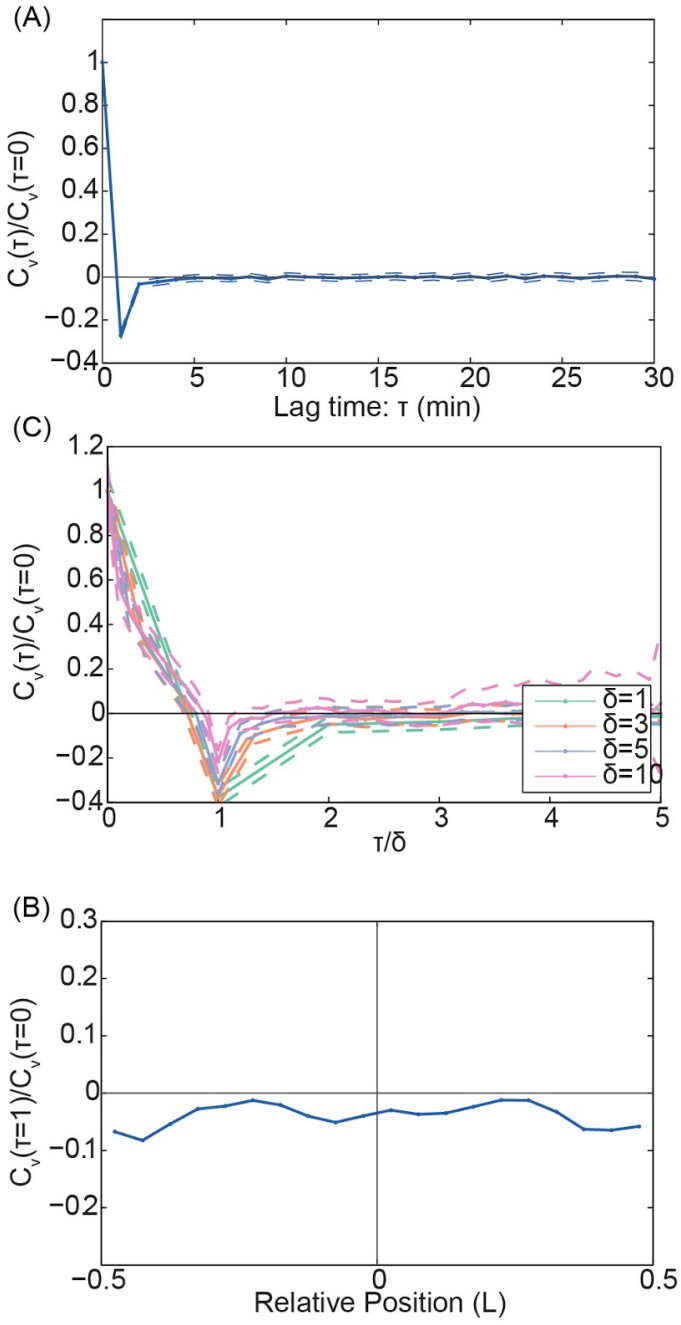

Figure S1. (A) Velocity Autocorrelation Function. Normalized velocity autocorrelation function defined as $C_V(\tau) = < v(t)\, v(t+\tau) >$ agrees with previous findings of the viscoelastic nature of the cytoplasm. **(B) Velocity Autocorrelation Function for**

different velocity lag times δ. The autocorrelation function collapses to 0.3 at the value of t/δ = 1 for different velocity lag times, where the velocity is defined as $v(t)$ = (v(t+δ)-v(t))/δ. This is in agreement with what has been predicted by the fractional Langevin motion model (1). **(C) Velocity Autocorrelation Function with relative cellular position.** Normalized velocity autocorrelation function for lag time of one minute shows velocity anticorrelation for all positions in cell.

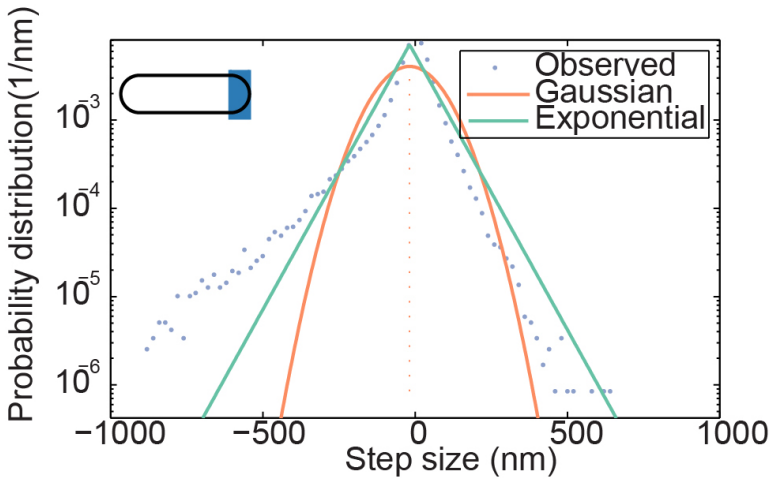

Figure S2. Step-size distribution has exponential tails. The step-size distribution (using the relative velocity model) is shown for MS2-mRNA complexes for a 1 minute lag time for complexes with starting position of their displacement vector near the old pole of the cell (⅕ of the cell), as illustrated in the inset. The data (blue circles) are compared with two models for the step-size distribution: *Exponential* (green line) and (ii) *Gaussian* (orange line). Both models have the same mean and variance as the experimental data. The observed step-size distribution shows the best agreement with an Exponential Model with tails of different decay constants because large steps towards the pole are mitigated by membrane exclusion forces from the pole.

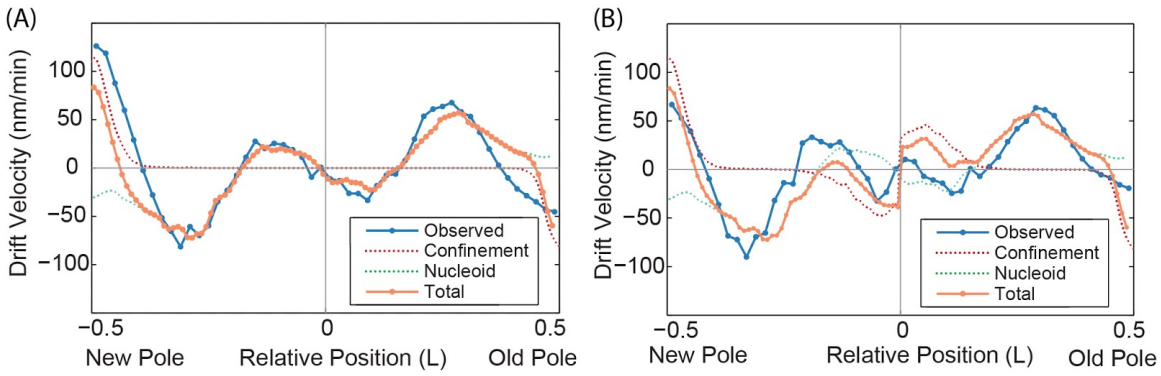

Figure S3. Panel A: First half of the cell cycle and predicted velocity profile. Measured velocity profile during the first half of the cell cycle (blue) and the predicted velocity profile (orange) of the combination of confinement at the poles from the inner membrane and nucleoid-exclusion versus relative cell position show excellent agreement. ***Panel B: Second half of the cell cycle and predicted velocity profile.*** Measured velocity profile during the last half of the cell cycle (blue) agrees with the combined predicted velocity profile (orange) of to membrane confinement at the poles, partial confinement at the middle due to septation and nucleoid-exclusion, successfully producing the split of the stable point at the middle of the cell.

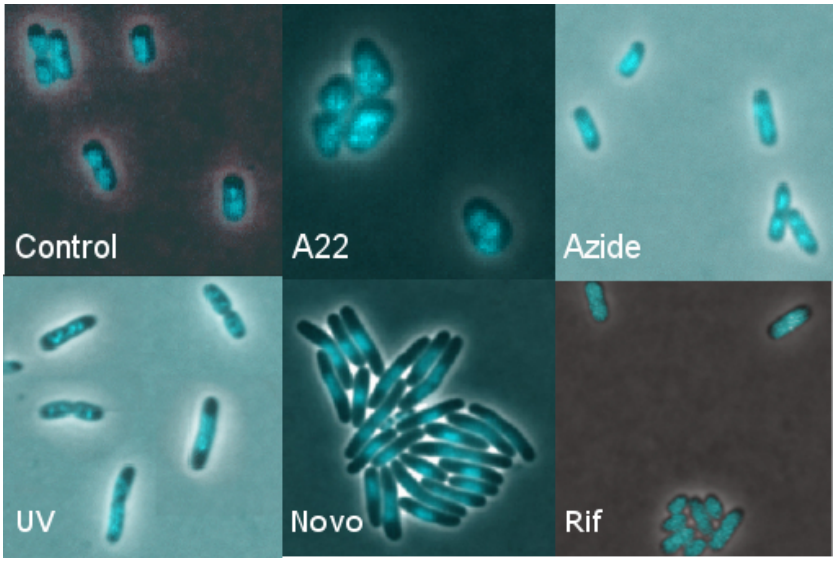

Figure S4. Nucleoid visualization of untreated and treated cells. Cells untreated and treated with either A22, Azide, Novobiocin, Rifampicin, and radiated with UV light and stained with DAPI for the visualization of the nucleoid. Cells treated with A22, show more diffusely localized nucleoids. Treatment with Novobiocin leads to condensation of the nucleoid. Cells radiated with Ultra Violet radiation appear to disperse the nucleoid around the cell. Rifampicin causes expansion of the nucleoid and Azide does not appear to cause a visible difference to the nucleoid's shape.

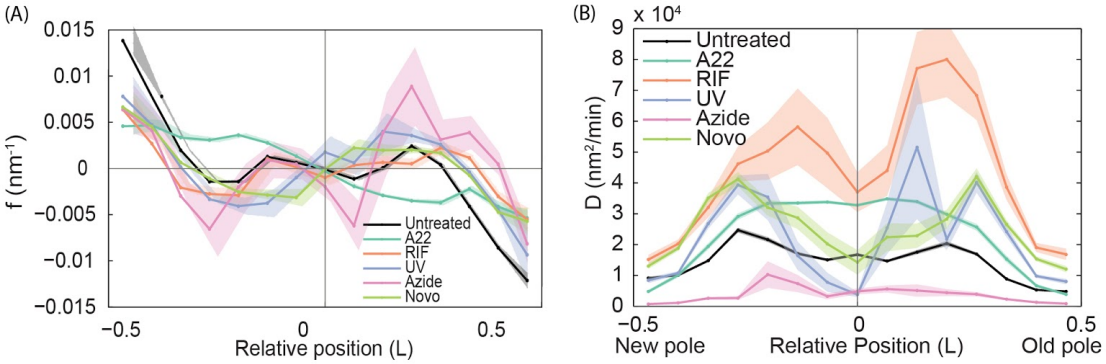

Figure S5: Panel A: Forcing ratio of untreated and treated cells. Forcing ratio (Drift Velocity / Diffusion Coefficient) of MS2-mRNA complexes with respect to the relative position in the cell in untreated, ATP-depleted (Azide), DNA-damaged (UV), gyrase inhibited (Novobiocin), transcription inhibited (Rifampicin) and spherical cells (A22). Inhibiting ATP hydrolysis and metabolic activity does not affect the shape of the forcing ratio curve. **Panel B: Spatial Dependence of diffusion coefficient of untreated and treated cells.** Diffusion Coefficient of MS2-mRNA complexes with respect to the relative position in the cell in untreated, ATP-depleted (Azide), DNA-damaged (UV), gyrase inhibited (Novobiocin), transcription inhibited (Rifampicin) and spherical cells (A22). Inhibiting ATP hydrolysis and metabolic activity decreases the complexes mobility whereas in all other cases the diffusion coefficient dramatically increased. The highest diffusion coefficient appears to be in the nucleoid occupied regions, especially at ¼ cell length.

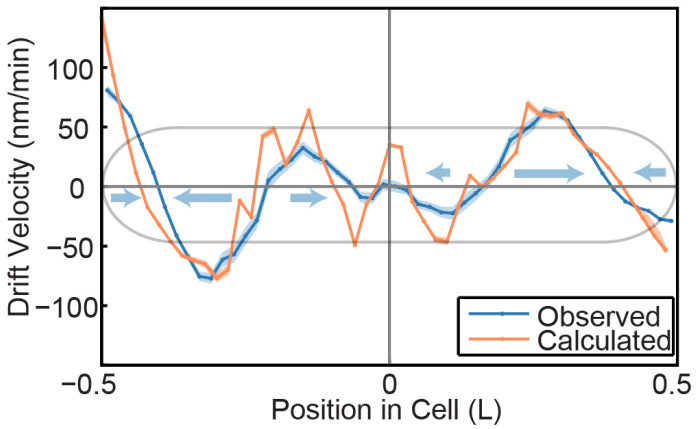

Figure S6. The calculated drift velocity profile using Eq. S1 assuming Fick's Law shows remarkable agreement with the observed drift velocity profile in the cell.

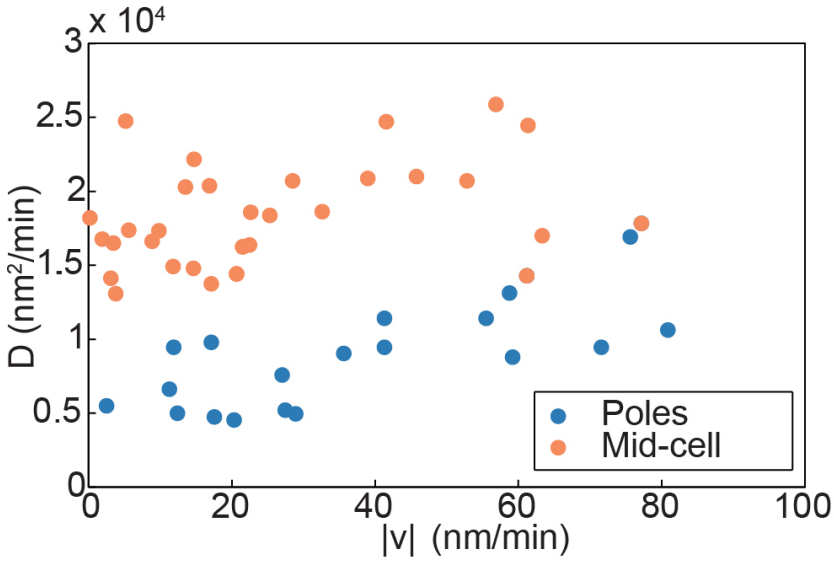

Figure S7: Scatter plot of diffusion coefficient versus drift velocity. The diffusion coefficient plotted against the magnitude of the drift velocity for each bin of subcellular position shows two subpopulations of particles, with fast and slow dynamics, according to their cellular position. Both regions show a similar distribution of drift velocities, but particles at the poles generally exhibit lower diffusion coefficients whereas particles at middle and quarter cell regions (Mid-cell) exhibit higher diffusion coefficients.

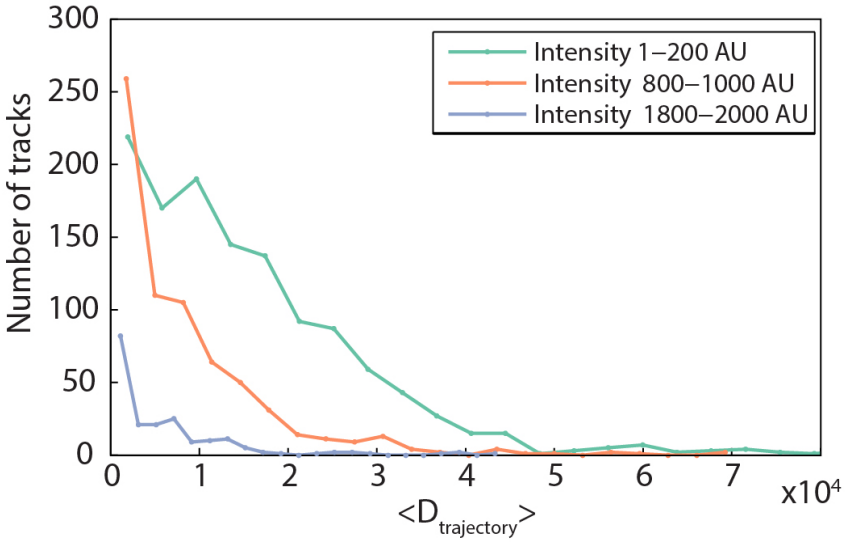

Figure S8: Mean diffusion coefficient as a function of MS2-mRNA focus intensity. To investigate whether or not focus intensity is a reliable measure of particle size, we plot a histogram of mean diffusion coefficient of each MS2-mRNA trajectory for three representative ranges of MS2-mRNA intensity (lowest, mid, and highest intensity used for analysis) in the first frame of the cell cycle. Through Stoke's Law, if intensity was proportional to particle size, we would expect the diffusion coefficient to scale inversely with the intensity of the focus. Instead, we observe a broad distribution of diffusion coefficients for all ranges of focus intensity. This is a consequence of complete cell cycle imaging and photobleaching: Because the MS2-mRNA complexes are not degraded, when they are inherited by daughter cells, they have been exposed to the lamp for varying amounts of time and thus photobleached for varying amounts of time. Therefore, in an experiment with complete cell cycle imaging, the intensity is not a reliable measurement of particle size.

SUPPORTING TEXT

S1. ***Agreement between observed drift velocity and drift velocity from Fick's law support that the system is in steady state***

As a test whether or not steady state statistical mechanics is an appropriate approximation for the dynamics of molecules in the cytoplasm, we calculated a theoretical drift velocity profile using Fick's Law. Under steady state conditions, the net the flux of complexes should be zero, thus

$$J = 0 = n_{mRNA} v_{drift} - D_{mRNA} \nabla n_{mRNA} \quad \text{(S1)}$$

where n_{mRNA} is the number density and D_{mRNA} is the diffusion constant of MS2-mRNA molecules, respectively. The number density was calculated from the full spatial distribution of complexes (Fig. 2A) and a spatially-dependent diffusion constant was estimated using the local mobility of complexes (Fig. 3B). The calculated drift velocity profile from Eq. S1 shows remarkable overlap with experimental data (Fig. S6), supporting the use of the Langevin approximation.

S2. Derivation of the excluded volume of the nucleoid model

The cytoplasm is modeled as a lattice where nucleoid DNA and MS2-mRNA cannot occupy the same site. We treat the nucleoid as a gas of independent blobs with local number density n_N. The relative reduction in the number of nucleoid configurations as a results of opening up volume ΔV for a protein complex is

$$Z(\Delta V) \approx Z(0)\, exp(-n_N \Delta V), \quad \text{(S2)}$$

where $Z(0)$ is the partition function in the absence of a complex volume ΔV. (Note that this can be understood as a consequence of the p dV term from the Helmholtz Free Energy.) Therefore, given an external number density n_N, we expect the number density of the mRNA complexes to be

$$n_{mRNA} \propto Z(\Delta V) \propto exp(-n_N \Delta V). \quad \text{(S3)}$$

For convenience, we normalize the observed DNA number density to one and we will assume the nucleoid blob density is related to the DNA density,

$$n_N = N_N n_{DNA}, \quad \text{(S4)}$$

where the constant of proportionality is the number of blobs N_N. We now define a unitless exclusion fraction:

$$\Phi \equiv \frac{N_N \Delta V}{V_{cell}}, \quad \text{(S5)}$$

where is the number of nucleoid blobs multiplied by the fraction of the cell volume excluded by the protein complex.

To understand the meaning of Φ it is useful to re-express it in terms of the total volume excluded by the crowding agent (DNA). We rewrite the volume of the ms2 complex (ΔV) in terms of the volume of an individual crowding agent δV where

$$\Delta V = r\,\delta V, \quad \text{(S6)}$$

and r is the number of statistically independent crowing agents excluded by an ms2-mRNA complex. Φ can then be written in terms of the total excluded volume of the nucleoid ($V_N = N_N \delta V$):

$$\Phi = \frac{V_N}{V_{cell}} r, \quad \text{(S7)}$$

where Φ depends on both the fraction of volume excluded and the number of statistically independent crowding agents excluded by the ms2 complex. A closely related result is derived in more detail in Ref 27, Chapter 14 by an alternative method. We note that r depends on the structure of the nucleoid and is therefore not know a priori even though the volume excluded by the chromosome is widely believed to be roughly 10-20% of the cell (12). Therefore the unitless constant must be fit to the data.

We can now rewrite the number density of the mRNA

$$n_{mRNA}(x) \propto Z(\Delta V) \propto exp(-\Phi V_{cell} n_{DNA}(x)), \quad \text{(S8)}$$

where the model for the mRNA number density is parameterized by a single parameter, the exclusion fraction Φ. We can use this relationship between the number density of mRNA and DNA to obtain a value for the unitless parameter Φ=1.9. Since the factor *r* can be quite large (e.g. Ref 27), this value appears to be consistent with our proposed

model.

It follows that the free energy associated with the excluded volume of the chromosome regions can be approximated as

$$G = -k_bT \log Z = -k_bT \log (exp(-\Phi V_{cell} n_{DNA})) \quad \text{(S9)}$$

We can estimate the effective external force caused by the chromosome unattainable regions to be

$$F = -\nabla G = -\Phi V_{cell} k_b T \nabla n_{DNA} \quad \text{(S10)}$$

Finally, from Fick's law the contribution of the DNA excluded volume to the drift velocity can be approximated to be

$$< v > (x,t) = \frac{<F>}{\gamma} = -\Phi V_{cell} D(x,t) \nabla n_{DNA}(x,t) \quad \text{(S11)}$$

S3. Derivation of membrane exclusion model.

To estimate the exclusion forces from membrane confinement at the cell poles, we treat the cell poles as hard-walls and explicitly solve the diffusion equation as a function of distance from the cell wall. Note that the solutions for each cell pole are symmetric, therefore we only show the solution for a single hard-wall but that the complete solution is a combination of the symmetric solutions. We begin by calculating the expectation value of the step-size distribution of a diffusive particle a distance δ from the wall:

$$< x - \delta > = \int_0^\infty dx\, (x-\delta)\rho(x,\delta) \quad \text{(S12)}$$

where $\rho(x,\delta)$ is a probability density function. The hard-wall condition can be represented using the method of images, where the probability density function is the sum of gaussians at $+\delta$ and $-\delta$:

$$< x - \delta > = \frac{1}{\sqrt{2\sigma^2\pi}} \int_0^\infty (x-\delta)(e^{-(x-\delta)^2/2\sigma^2} + e^{-(x+\delta)^2/2\sigma^2}) dx\,. \quad \text{(S13)}$$

In the case of 1D-diffusive motion with diffusion constant *D*, the standard deviation of the gaussians are defined as $\sigma^2 = 2D\Delta t$, where Δt is the lag time between successive measurements. This integral can then be solved exactly:

$$< x - \delta > = \sqrt{\frac{4D\Delta t}{\pi}}\ exp(-\frac{\delta^2}{4D\Delta t}) - \delta(1 - erf(\frac{\delta}{\sqrt{4D\Delta t}}))\,. \quad \text{(S14)}$$

To estimate the drift velocity profile from membrane confinement, we use the same convention that we use for experimental data and divide the step size distribution by the lag time between successive measurements:

$$< v > \; = \frac{1}{\Delta t} \sqrt{\frac{4D\Delta t}{\pi}} \; exp(-\frac{\delta^2}{4D\Delta t}) - \frac{\delta}{\Delta t}(1 - erf(\frac{\delta}{\sqrt{4D\Delta t}})) \quad \text{(S15)}$$

Section S4. Biased diffusive motion.

A standard approach to characterize the stochastic motion of a diffusive particle in the presence of a biasing force is to calculate the mean squared displacement (MSD),

$$MSD(t) \equiv \; < (x(t) - x(0))^2 > . \quad \text{(S16)}$$

In an ideal Newtonian fluid, the MSD of an object undergoing diffusive motion with a constant biasing force takes the following form:

$$MSD(t) \; = \; 2\,D\,t \; + (v\,t)^2, \quad \text{(S17)}$$

where D is the diffusion coefficient, v is the bias velocity, and t is the observation time. At short times the MSD is dominated by diffusive motion (first term) and at long times the motion is dominated by the bias velocity (second term). The bias velocity explicitly depends on the model of motion (*absolute* versus *relative*) while the diffusion coefficient is independent of the model. Because each term in Eq. 3 scales differently with time, the differences between the two velocity models are irrelevant at short times whereas at long times the models are expected to be divergent, according to their bias velocity. We therefore propose to determine which model best represents the behavior of MS2-mRNA complexes by identifying the velocity model that has the smallest MSD and therefore the smallest bias.

We can also estimate a timescale at which the bias velocity dominates over the diffusive motion by setting the two terms in Eq. S17 equal to each other. The timescale at which the bias velocity dominates the motion, $t \sim 2D/v^2$, for our experimental values of $D \sim 10^4$ nm^2/min and $v \sim 50$ nm/min is approximately 10 minutes, which is consistent with the timescale that absolute model diverges from the relative model in Fig. 2(B).

SUPPORTING REFERENCES

(1) Weber, S. C., Thompson, M. A., Moerner, W. E., Spakowitz, A. J., & Theriot, J. A. (2012). Analytical tools to distinguish the effects of localization error, confinement, and medium elasticity on the velocity autocorrelation function.*Biophysical journal*, *102*(11), 2443-2450.